Catalysis Today 213 (2013) 9–17

Contents lists available at SciVerse ScienceDirect

Catalysis Today

journal homepage: www.elsevier.com/locate/cattod

Deoxygenation of m-cresol on Pt/γ-Al_2O_3 catalysts

M.S. Zanuttini, C.D. Lago, C.A. Querini*, M.A. Peralta

Instituto de Investigaciones en Catálisis y Petroquímica (INCAPE) (FIQ, UNL, CONICET), Santiago del Estero 2654, 3000 Santa Fe, Argentina

ARTICLE INFO

Article history:
Received 17 December 2012
Received in revised form 10 April 2013
Accepted 12 April 2013
Available online 15 May 2013

Keywords:
Deoxygenation
Bio-oil
Cresol
Platinum
Alumina

ABSTRACT

In this work the deoxygenation of m-cresol, used as a bio-oil model compound, was studied at atmospheric pressure, using Pt/γ-Al_2O_3 catalysts. The main products obtained in this system were toluene, benzene and methylcyclohexane. Possible reaction routes for cresol deoxygenation were proposed. The influence of the metal loading, H_2/cresol ratio and temperature on products distribution was analyzed. Catalyst deactivation was studied by TPO. The catalysts were characterized by XPS, XRD, BET, TPR, and TEM. Product distribution is explained based on the relative rates of cresol dehydroxylation and demethylation, which leads to toluene and phenol formation, respectively. High selectivity to toluene was obtained with the catalyst with the higher metal loading (1.7 wt.%), while in the case of low metal loading (0.05 wt.%) high yields of light hydrocarbons were obtained. Coke deposition took place preferentially on the metal particles and could be removed by treatment at low temperatures, e.g. 350 °C. This catalyst displays a very good activity and selectivity towards toluene formation at mild temperature (300 °C) and atmospheric pressure, which is a better performance than that already reported for other catalysts.

1. Introduction

The lignocellulosic biomass fast pyrolysis is one of the possible alternatives to generate biofuels. The liquid product obtained in this process is called bio-oil. Although it is a potential fuel, it cannot be used as such without prior refining due to its high viscosity, low heating value, corrosiveness and instability [1,2]. Moreover, the high reactivity complicates the use of bio-oil as a fuel and its long term storage. The refining essentially involves the removal of oxygen, since it imparts to this biofuel the undesirable properties mentioned above [3]. Bio-oil deoxygenation has been studied using hydrotreating catalysts at high pressures of hydrogen or a mixture of hydrogen and carbon monoxide, and/or in the presence of hydrogen donor solvents [4–9]. Acid catalysts such as zeolites or silica-alumina, working at low pressures were also used [10–15]. However, when studying deoxygenation reactions using model compounds with different types of catalysts it was generally observed that the phenolic fraction was not deoxygenated or it required a high hydrogen consumption and high pressure. Besides, when using high hydrogen pressures, the formation of fully hydrogenated products of lower octane number and therefore, less important in order to feed the fuel pool, was generally observed. Several catalysts, mostly hydrotreating catalysts, were used to deoxygenate phenolic compounds at high hydrogen pressures. Table 1 presents the catalysts used at high H_2 pressure, and relevant information recently reported in this field. Phenolic compounds represent an important fraction of the bio-oil. There are few reports in which good results are presented, related to the deoxygenation of these compounds with low hydrogen consumption (atmospheric pressure) and high selectivities to high octane deoxygenated aromatics. For example, phenol was deoxygenated with high selectivity to benzene, at atmospheric pressure with the Ni/SiO_2 catalyst [26]. On the other hand, results obtained in the deoxygenation of phenol, 2-methoxy-4-(2-propanyl) phenol and other phenolic compounds using HZSM-5 catalysts were not satisfactory [27–30]. The Fe/SiO_2 catalyst [31] was used to deoxygenate guaiacol but the selectivity to benzene–toluene–xylenes fraction (BTX) was low. Guaiacol was also deoxygenated with Pt–Sn [32] and V_2O_5/Al_2O_3 catalysts [33], but phenol was the main product in both cases. Recently, Resasco et al. [34] reported the used of gallium modified beta-zeolite for hydrodeoxygenation of m-cresol, working at low pressures (1 atm), but at rather high temperatures, in the range of 400–550 °C. Total conversion of m-cresol was obtained at W/F = 24, with a toluene yield of 40%.

In sum, previous reported research related to bio-oil deoxygenation was not completely successful mainly due to two reasons. On one hand, when working under conditions of low hydrogen pressure with acid catalysts, a high bio-oil fraction was not deoxygenated. This fraction was formed mainly by phenolic compounds. On the other hand, in order to deoxygenate the phenolic fraction, high hydrogen consumption was required and completely

* Corresponding author at: Santiago del Estero 2654, (3000) Santa Fe, Argentina. Tel.: +54 342 4533858; fax: +54 342 4531068.
E-mail address: querini@fiq.unl.edu.ar (C.A. Querini).

0920-5861/$ – see front matter © 2013 Elsevier B.V. All rights reserved.
http://dx.doi.org/10.1016/j.cattod.2013.04.011

Table 1
Deoxygenation of phenolic compounds at high H_2 pressure.

Catalyst	Reagent	Main products	*P* (MPa)	Ref.
MoS_2, CoMoS	Guaiacol	Cyclohexane, cyclohexene and benzene	4	[16]
Co–Mo–B	Phenol	Cyclohexane	4	[17]
$NiMoP/Al_2O_3$	2-ethylphenol	Ethylcyclohexane	7	[18]
$CoO–MoO_3/Al_2O_3$ sulfided	Cresol	Toluene and methylcyclohexane	6.9	[19]
$MoO_3–NiO/Al_2O_3$	Phenol	Benzene, cyclohexane and methylcyclopentane	2.8	[20]
$Rh/SiO_2–Al_2O_3$, $Ru/SiO_2–Al_2O_3$	Guaiacol	Toluene and methylcyclohexane	4	[21]
NiMo sulfide	Phenol	Benzene, cyclohexane, cyclohexene	2.8	[22]
MoS_2, $CoMoS_2$	Phenol	Benzene, cyclohexane, cyclohexene	2.8	[23]
$Ni,Mo/Al_2O_3$, Mo/Al_2O_3, $Co,Mo/Al_2O_3$,	2-ethylphenol	Ethylcyclohexane, ethylbenzene	7	[24]
CoMoS	Guaiacol	Benzene, toluene, methylcyclohexane, methylcyclohexene	4	[25]

hydrogenated products were usually obtained. Lobo et al. [48,49] studied the deoxygenation of m-cresol using platinum supported on alumina, at 260 °C and a $W/F = 0.58\ g_{cat}h/g_{cresol}$, and proposed a reaction sequence in which the m-cresol is hydrogenated on the metal, dehydrated on the acid sites (alumina) and finally dehydrogenated on the metal. The catalyst used by Lobo et al. [48] was bifunctional, with the metal being active in hydrogenation–dehydrogenation and hydrogenolysis reactions, and the acid mainly in dehydration and hydrocraking reactions. B. Subramaniam et al. [50] compared Pt/Al_2O_3 with other supported metal catalysts in m-cresol conversion in liquid phase, and found that Pt was more active than the other catalysts.

In this work, the deoxygenation of cresol (methyl·phenol) was studied in conditions of low hydrogen pressure using $Pt/\gamma\text{-}Al_2O_3$ catalysts. These catalysts were chosen after a screening of different types of catalysts comprising acid zeolites, different oxides, transition metals and noble metals. m-Cresol was chosen as a bio-oil model compound corresponding to the phenolic fraction. The effect of operative variables on the catalytic activity, selectivity to different deoxygenated products and catalyst stability was analyzed, and possible reaction routes were proposed.

2. Experimental

2.1. Catalysts preparation

The catalysts were prepared by wet impregnation of platinum precursor on $\gamma\text{-}Al_2O_3$ support. Tetraammonium platinum (II) nitrate (metal content 50%) was supplied by Alfa Aesar. An aqueous solution of 1% of $Pt(NH_3)_4(NO_2)_3$ was used to prepare the catalyst. A suspension of $\gamma\text{-}Al_2O_3$ in the metal precursor solution was stirred on a hot plate at 110 °C until complete evaporation. The impregnated catalyst was dried in an oven at 110 °C for 12 h. The dried sample was calcined in an electric furnace at 350 °C for 2 h. Platinum content was varied between 0.05 and 1.7 wt.%.

2.2. Catalysts characterization

BET surface areas were obtained using a Quantachrome Autosorb 1 analyzer. Pore volumes were estimated by means of the *t*-plot.

Catalysts crystalline structures were characterized by X-ray diffraction (XRD). The X-ray diffractograms were obtained with a Shimadzu XD-D1 instrument with monochromator using CuKα radiation at a scanning rate of $4\ ^\circ min^{-1}$, from $2\theta = 5^\circ$ to 100°.

Reducibility of metallic catalysts was studied by temperature-programmed reduction (TPR). Temperature-programmed reduction (TPR) experiments were performed employing an OKHURA TP-2002 S system, equipped with a thermal conductivity detector (TCD) detector. TPR runs were carried out with a heating rate of $10\ ^\circ C\ min^{-1}$ in 5% H_2/Ar ($30\ mL\ min^{-1}$). The temperature was increased from 20 °C to 900 °C.

Particle size distributions were determined by Transmission Electron Microscopy (TEM). The reduced samples were placed in distilled water. One drop of this suspension was then placed on holey carbon supported on a copper grid. The micrograph images of the samples were acquired with a JEOL 100 CX model microscope at 100 kV, and a magnification of 450,000 ×. The metallic dispersions were calculated by the following equations [35,36]:

$$d_{Pt} = \frac{0.821}{D_{Pt}} \quad (1)$$

where D_{Pt} is the metallic dispersion and d_{Pt} is the particle size (D_{va}) in nm. D_{va} is a volume-area average size defined as follows:

$$D_{va} = \frac{\sum n_i d_i^3}{\sum n_i d_i^2} \quad (2)$$

The amount of carbonaceous materials deposited on the spent catalysts were determined by Temperature-Programmed Oxidation (TPO), using a stream of 5% (v/v) O_2 in N_2 and a heating rate of $12\ ^\circ C.min^{-1}$. The oxidation products were detected with a flame ionization detector (FID) after methanation. Further details can be found elsewhere [37].

The Pt dispersion was also determined by CO pulse chemisorption. Dynamic CO pulse chemisorption measurements were carried out by sending 250 μL pulses of 1% CO/He on reduced samples. CO was detected with a FID, after quantitative methanation in a Ni/kieselghur catalyst at 400 °C, which largely improves the sensitivity.

The chemical state of Pt was determined by X-ray Photoelectron Spectroscopy (XPS). The XPS analyses were performed in a multitechnique system (SPECS) equipped with a dual Mg/Al X-ray source and a hemispherical PHOIBOS 150 analyzer operating in the fixed analyzer transmission (FAT) mode. The samples were mounted on a sample rod, placed in the pretreatment chamber of the spectrometer, submitted to a reduction in H_2/Ar during 10 min, and then evacuated at room temperature. The spectra were obtained with pass energy of 30 eV. The spectra were processed using the software Casa XPS (Casa Software Ltd., UK). The intensities were estimated by calculating the integral of each peak after subtracting a Shirley-type background and fitting the experimental curve to a combination of Lorentzian and Gaussian lines. Bending energy values were referred to the C1 peak (284.6 eV). For the quantification of the elements, sensitivity factors provided by the manufacturers were used.

2.3. Catalytic activity

The catalytic activity was measured at atmospheric pressure in a continuous-flow fixed-bed reactor, made of 5 mm internal diameter quartz tube. The catalyst bed was supported with quartz wool. Above the catalytic bed, quartz beads were loaded in order to improve the heat transfer. The catalyst was pretreated under flow of H_2 ($30\ ml\ min^{-1}$) by heating at $10\ ^\circ C\ min^{-1}$ from room temperature

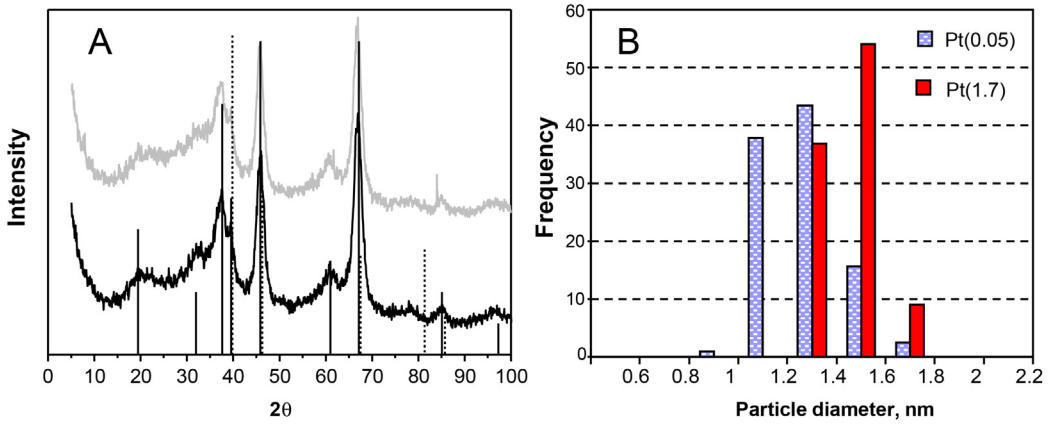

Fig. 1. (A) XRD patterns of fresh Pt (1.7%)/γ-Al_2O_3 catalyst (grey) and γ-Al_2O_3 (black). JCPDS-ICDD characteristic signals for Pt (dash line) and γ-Al_2O_3 (solid line). (B) TEM results, histograms of Pt (1.7%)/γ-Al_2O_3 and Pt(0.05)/γ-Al_2O_3.

to 300 °C or 500 °C and maintained at this temperature for 1 h. The catalyst was then cooled down to the reaction temperature (200–450 °C). The carrier was bubbled in liquid cresol maintained at a preselected temperature in the range 55–90 °C, in order to saturate the gas. The carrier flow rate was 5–50 ml min^{-1}. Under these conditions the cresol partial pressure in the gas stream fed to the reactor was between 0.51 and 107.2 Torr, and the contact time (W/F) was between 0.1 and 38 g_{cat} h $(g_{cresol})^{-1}$. After each run, the catalyst bed was purged with H_2 at the reaction temperature during 30 min. Experiments feeding a mixture of cresol and phenol, were also carried out. In this case, the mixture was fed by a syringe pump (Apema). The gas flow rates were controlled with mass flow controllers (Aalborg Instruments and Controls, Inc.,). The reactor outlet stream was analyzed in a GC (SRI 8610) connected online and equipped with a ZB-5 capillary column (15 m) and FID detector. A split ratio of 100 was used. Standard samples were used in order to identify the reaction products. In addition, a GC–MS (Varian Saturn 2000) equipped with a HP-5 capillary column was used to identify the reaction products collected in a condenser cooled at 0 °C. The non-condensed gases were analyzed by GC using a Petrocol (Supelco) capillary column (100 m).

In order to evaluate catalytic activities at different contact times, the W/F was varied between 37.7 and 11.3 g_{cat} h $(g_{cresol})^{-1}$ changing the catalyst mass loaded in the reactor and maintaining the hydrogen flow rate and the saturator temperature constant. Values of W/F lower than 11.3 g_{cat} h $(g_{cresol})^{-1}$ were obtained by increasing the cresol flow rate and maintaining the catalyst mass constant.

The selectivity of catalysts with different Pt contents were compared at conversions near 80%, which was obtained changing the W/F between 80 and 0.1 g_{cat} h $(g_{cresol})^{-1}$.

Conversion levels and product yields at different temperatures were analyzed with Pt(1.7)/γAl_2O_3 catalysts. The experiments were carried out with the same catalyst sample, increasing the temperature from 200 °C to 450 °C, in 50 °C steps. Afterwards the reactor was progressively cooled down, following the reverse procedure, using the same temperature values to determine the catalytic activity. This procedure was adopted to check the catalyst stability by comparison of the activities obtained in the direct and the reverse temperature sequence.

The absence of internal and external mass transfer limitations was verified using different catalyst particle sizes (W/F = 0.4 g_{cat} h $(g_{cresol})^{-1}$), and H_2 flow rates (5.5 and 50 cm^3/min) at two different W/F (W/F = 0.15 and 37 g_{cat} h $(g_{cresol})^{-1}$). Under these conditions, which are the extremes values used in this study in each variable, similar conversions and product distributions were obtained. No heat-transfer limitations are expected since the heats of reaction are relatively small.

Two sets of experiments corresponding to W/F = 0.48 g_{cat} h $(g_{cresol})^{-1}$ and W/F = 38 g_{cat} h $(g_{cresol})^{-1}$ were repeated 5 times. A good reproducibility was achieved. Relative standard deviation of product yields was 8%.

3. Results and discussion

3.1. Catalysts characterization

Fig. 1A shows the diffractograms corresponding to pure alumina, and to the Pt(1.7%)/γ-Al_2O_3 catalyst. JCPDS-ICDD characteristic signals for Pt (dash lines) and γ-Al_2O_3 (solid lines) are included. The X-ray diffractogram presents the typical signals of the γ-Al_2O_3 at 2θ = 45.901 °, 67.093 °, 37.635 °, 39.524 °, and 19.466 ° (JCPDS-ICDD 10-425). No signals corresponding to Pt crystals were observed. The diffractograms obtained with the catalysts are equal to those obtained with the support, what indicates that the metal particles are small. In the equipment used to obtain these results, the minimum Pt size that displays signals in the XRD spectrum is approximately 50 Å.

Fig. 1B shows the histograms that correspond to the Pt(1.7%)/γ-Al_2O_3 and Pt(0.05%)/γ-Al_2O_3. It can be observed that the Pt is highly dispersed in all samples, with particles diameter in the order of 14 Å. However, even though the mean particle size is not very different between the Pt(1.7%) and Pt(0.05%) catalysts, there is an evident difference in the amount of smaller particles. The catalyst with 0.05% Pt has an important fraction of particles with diameter below 1.2 nm. Nevertheless, the difference in the Pt particles size is not significantly different between these two catalysts.

The TPR profile of Pt(1.7)/γAl_2O_3 (not shown) displayed two peaks, one at 240 °C and the second at 414 °C, which can be assigned to the bulk phase of the PtO_x and to highly dispersed particles with strong interaction with the support, as previously reported [38–40].

Results of surface area, pore volume and pore diameter are shown in Table 2. The γ-Al_2O_3 catalytic surface area was 200 m^2 g^{-1}. The preparation procedure had little effect on the BET area, the pore volume, and pore diameter, and consequently, it can be expected that the activity results are not influenced by these negligible changes.

3.2. Effect of reduction temperature

The platinum catalysts were reduced at 300 and 500 °C. The activity results obtained in both cases were very similar (results not shown). Because of this, throughout this study results obtained with the catalysts reduced at 300 °C are presented.

Table 2
Metallic particle sizes, calculated dispersions, BET surface, pore volume (Vg) and average pore diameter (dp) values for the fresh catalysts.

Catalyst	TEM particle size, D_{va} (nm)	Calculated dispersion (%)	BET, Sg ($m^2\,g^{-1}$)	V_g ($ml\,g^{-1}$)	d_p (Å)
Pt(1.7%)/γ-Al_2O_3	1.50	67	214.0	0.488	87.7
Pt(0.5%)/γ-Al_2O_3	1.43	80	195.0	0.490	87.8
Pt(0.1%)/γ-Al_2O_3	1.41	80	189.6	0.492	87.9
Pt(0.05%)/γ-Al_2O_3	1.33	86	193.1	0.462	88.7

Table 3
XPS results.

		Activation temperature	
		300 °C	500 °C
Binding energy Pt $4d_{5/2}$ (eV)	314.0	314.1	
	316.9	317	
%	Pt^0	54.7	59.0
	PtOx	45.3	41

3.3. XPS studies

Fig. 2 shows the XPS spectra obtained with the Pt(1.7%)/γ-Al_2O_3 catalyst after reduction at 300 and 500 °C. Although the most intense photoemission lines of platinum are those arising from the 4f levels, this energy region is overlapped by the Al 2p line of γ-Al_2O_3. Therefore, in this article the Pt 4d line was used. This one is weaker but it is not overlapped by spectral lines of other components. This assignment of the Pt oxidation state is difficult and the information in literature is contradictory [41,42]. The low levels of Pt in the samples, along with the broad nature of Pt 4d features, introduce considerable uncertainty in the determination of binding energies. Fig. 2 presents the spectral region of Pt $4d_{5/2}$ line with substration of a Shirley background spectrum of Pt(1.7%)/Al_2O_3 reduced one hour at 300 °C and at 500 °C. The decomposition of the spectra to individual components revealed the presence of two platinum states: the reduced state (Pt°) with a binding energy (E_b) of 314.0–314.1 eV and the oxidized state with a E_b of 316.9–317 eV. Table 3 gives the Pt $4d_{5/2}$ binding energies observed in the samples after reduction at 300 and at 500 °C, and the percentages of the different states of platinum. These results show that there are no significant differences between the two treatments. As stated by Serrano-Ruiz et al. [41], even after reduction at 500 °C, Pt seems to maintain some δ^+ character, although this oxidation might occur also during the analysis. These analyses explain the activity results that showed that the cresol conversion and product distribution were practically the same with both pretreatments.

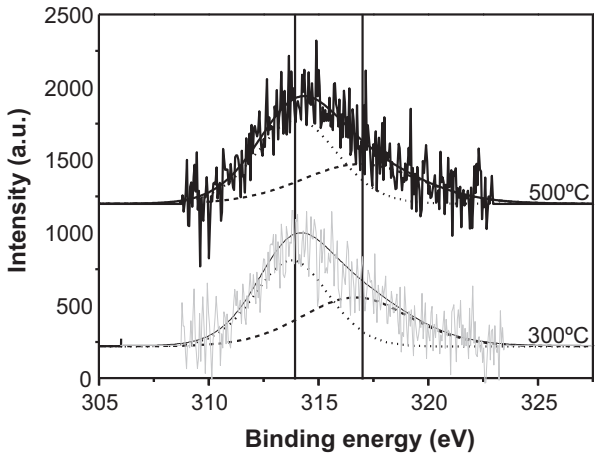

Fig. 2. Pt 4d spectra obtained by XPS for fresh Pt(1.7%)/γ-Al_2O_3 catalyst reduced at 300 °C (grey) and at 500 °C (black).

3.4. Catalytic activity

A blank experiment was carried out at 500 °C without catalyst in order to determine conversion due to thermal decomposition. In this case, only cresol was observed at the reactor outlet. Pure alumina was tested at 300 °C, W/F = 11.3 h, and H_2/HC = 510. In this case, the m-cresol conversion also was zero. The amount of coke deposits detected by TPO analysis was 5.14%, with a maximum in the TPO profile at 490 °C. Nevertheless, the alumina had a light-pink colour after the reaction, while the coked catalysts were grey or black, what indicates that there is a different nature of the coke deposits between the alumina and the Pt/Al_2O_3 catalysts. It is very interesting to highlight, that the amount of coke deposited on alumina is five times higher than that on Pt(1.7)/Al_2O_3, what demonstrates the importance of the metallic function not only in changing the relative rates of the reactions involved in this system, but also in the coking mechanism. Evidently, the fast deoxygenation that occurs on the metal function leading to the formation of toluene (as will be shown in the following sections) and the hydrogen spillover, lead to an important improvement in the catalyst stability.

The conversion and yields of products vs. time on stream (TOS) for different contact times (W/F) are shown in Fig. 3 for m-cresol deoxygenation at 300 °C. The main reaction products were toluene (Tol), benzene (Bz), methylcyclohexane (MCH) and light hydrocarbons (LH) including mainly methane, ethane, propane, butane, and small amounts of *n*-pentane, isopentane, 2 and 3 methylhexane and hexane. Phenol (Ph) was found in very low amounts. GC–MS analyses of the condensed samples confirmed the GC products identification. Methylcyclohexanol and methylcyclohexene were not observed. Small amounts of dimethyl phenyl, dimethyl diphenyl, and a dimethyl benzophenone were also observed by GC–MS. The conversion was lower than 100% only in the case of W/F = 0.15 $g_{cat}\,h\,(g_{reactant})^{-1}$. These results are in good agreement with the conversion reported by Lobo et al. [48], who found that at 260 °C and W/F = 0.58 $g_{cat}\,h\,(g_{reactant})^{-1}$ using Pt(1.7 wt.%)/Al_2O_3 catalyst, the conversion was 38%.

A mixture of 50 wt.% phenol and 50 wt.% cresol was used in order to elucidate the reaction path for benzene formation. If benzene comes from toluene and from phenol, the benzene/toluene ratio would be higher when feeding the mixture of phenol plus cresol, since the only source of toluene is cresol. The contact time (W/F) for this experiment was 0.1 $g_{cat}\,h\,(g_{reactant})^{-1}$. The conversion levels and the benzene/toluene ratio corresponding to both feeds, i.e., cresol and the mixture phenol-cresol, obtained with Pt(1.7)/γAl_2O_3, are shown in Fig. 4A and B. The conversion as a function of time followed the same behaviour for both feeds. However, the benzene/toluene ratio was much higher when feeding the mixture of cresol and phenol, confirming that benzene was formed by dehydroxylation of phenol at a high rate. Since the amount of benzene is rather small under all the reaction conditions with m-cresol, another important conclusion that can be drawn from these results is that phenol formation rate on the Pt/γAl_2O_3 catalysts is much slower than the cresol dehydroxylation rate that forms toluene. This is a very important result to be highlighted, since the selectivity towards deoxygenated products would be very high. These results also indicate that the transalkylation of m-cresol forming

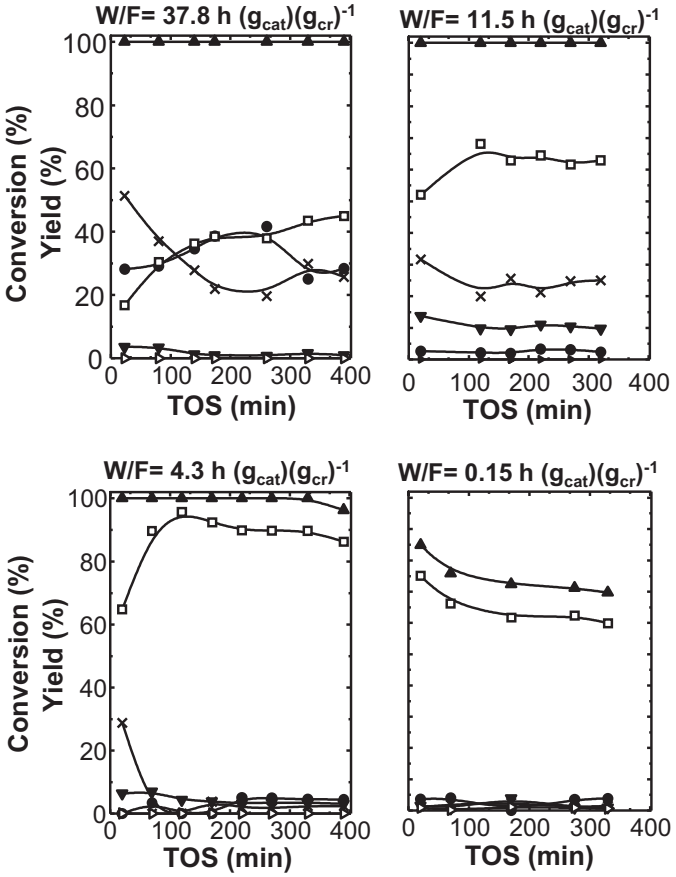

Fig. 3. Cresol conversion and product yield vs. time on stream for different contact times (W/F) over Pt(1.7%)/γAl_2O_3 at 300 °C. References: (▲) m-cresol conversion, (□) toluene, (×) LH, (▼) benzene, (▷) phenol, and (●) methylcyclohexane.

phenol and dimethylphenol does not occur at an appreciable rate due to the weak acidity of the alumina, in contrast to the result obtained with a high acidity catalyst [43].

Benzene formation from phenol could occur by dehydration on the acid sites of the alumina, and by CO bond hydrogenolysis on the metal. There are not direct evidences regarding which site is more active under the conditions used in these experiments. However the fast change in the benzene/toluene ratio shown in Fig. 4B, and the low amount of coke deposited on the alumina as will be shown below, suggests that the metal is playing an important role. Nevertheless, this issue needs further studies.

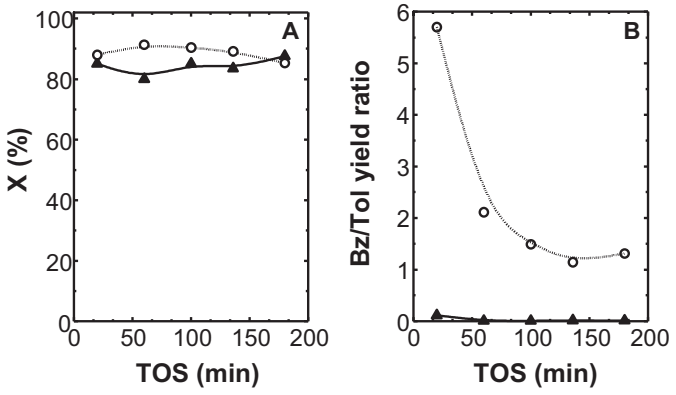

Fig. 4. (A) Cresol conversion; (B) benzene–toluene yield ratio; Feed: (▲) cresol; (○) phenol:cresol (1:1) mixture, Catalyst: Pt (1.7%)/γAl_2O_3 at 300 °C, H_2/m-cresol molar ratio = 100, W/F = 0.1 $g_{cat}\,h\,(g_{reactants})^{-1}$.

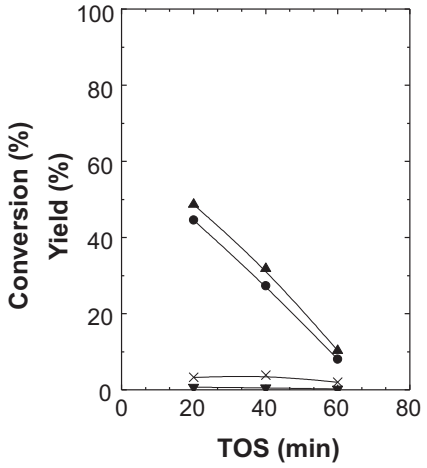

Fig. 5. Toluene conversion and product yield vs. time on stream. Pt(1.7%)/γAl_2O_3, at 300 °C, H_2/toluene molar ratio = 50, W/F = 0.1 $g_{cat}\,h\,(g_{reactants})^{-1}$. References: (▲) toluene conversion, (×) LH, (▼) benzene, (▷) phenol, and (●) methylcyclohexane.

Table 4
Coke content on spent catalysts obtained by TPO.

Catalyst	W/F $g_{cat}\,h\,(g_{cresol})^{-1}$	H_2/cresol molar ratio	TPO%C
Pt(1.7%)/γ-Al_2O_3	0.15	65	1.93
	4.3	197	1.19
	11.3	510	1.05
	37.7	510	0.39

Toluene was fed in another experiment, with the Pt(1.7)/γAl_2O_3 catalyst, in order to investigate the other possible reaction path for benzene formation, and also for methylcyclohexane production. The experimental conditions were T = 300 °C and W/F = 0.1 $g_{cat}\,h\,(g_{reactant})^{-1}$. Fig. 5 shows the results. Methylcyclohexane was the main product. This result indicates that the Pt(1.7)/γAl_2O_3 catalyst was more selective to ring hydrogenation than hydrocracking under these reaction conditions, in agreement with results obtained in the hydrogenation of phenol [43].

Coke deposits were determined by TPO analyses of the spent catalysts. Two maxima were observed in all the TPO profiles, around 250 °C and 450 °C respectively (not shown). The first peak is sharp, with a width of 50 °C. These two maxima correspond to carbon deposited on the metal or near the metal particles and on the support, respectively [44–46]. The carbon contents on the spent Pt(1.7)/γAl_2O_3 catalyst as a function of the space velocity are summarized in Table 4. The H_2/cresol ratio was not constant in these experiments. However, the last two points shown in the table have the same H_2/cresol ratio, with higher amount of coke deposited at shorter contact time, indicating that the deactivation follows a parallel mechanism, with the coke being formed faster from cresol than from the products. Most probably, the compounds deposited on the catalyst are products of cresol condensation, similar to the dimethyl benzophenone, detected in low amounts. The other compounds present in the system, either oxygenated or not, leads to the formation of coke, as it has been determined years ago in the study of deactivation of reforming catalysts. Nevertheless, the relative rates of coke formation is very different among these hydrocarbons, and according to the results shown above, the cresol is the main precursor. Nevertheless, since these data was obtained at 100% conversion, additional information is needed in order to determine the exact mechanism for coke deposition.

3.5. Effect of metal loading on product distribution

The cresol deoxygenation reaction was evaluated with different Pt loadings. Toluene is a preferred product compared to

Table 5
Products distribution obtained with different catalyst. W/F = 37.7 $g_{cat}\,h\,(g_{reactants})^{-1}$, H_2/cresol molar ratio = 510. Temperature: 300 °C.

%Pt	Conversion	MCH	LH	TOL	Bz	MCH/Tol
0.05	100	3.27	45.9	46.4	4.04	0.08
0.1	100	3.83	41.8	51.2	3.02	0.07
0.5	100	4.61	36.7	56.8	1.85	0.07
1.7	100	5.71	6.88	86.11	1.28	0.07

Table 6
Products distribution obtained with different catalysts. Temperature: 300 °C.

%Pt	Conversion	MCH	LH	TOL	Bz	MCH/Tol	H_2/Cresol
0.05	82.0	1.0	71.3	8.0	0.0	0.125	1483
0.1	90.0	2.0	55.1	22.0	10.9	0.091	1483
0.5	74.0	4.4	1.8	66.7	1.1	0.066	197
1.7	83.5	3.7	1.1	77.2	1.5	0.048	65

methylcyclohexane since it has a higher octane number. The Pt loadings used in these experiments were 1.7%, 0.5%, 0.1%, and 0.05%. The activity results are summarized in Table 5. All the catalyst reached 100% conversion, what shows the very high activity of this catalyst for m-cresol conversion. The catalyst with the lower metal loading produced a significant amount of light hydrocarbons, as compared to the catalyst with 1.7% Pt, consequently, the toluene yield was much lower in the former. As above described, the catalyst with 0.05%Pt has smaller particles. It has been reasonably established, that the smaller the metal particle, the higher the hydrogenolytic activity, nevertheless, the difference in size among the catalysts was not large enough to explain the different product distribution observed with each of them. On the other hand, the catalyst with the higher Pt loading has a much higher ratio of metal/acid sites. Consequently, the relative rates of the reactions involved in the mechanism for cresol conversion are different, thus affecting the product distribution. As the metal content increases, the metal-catalyzed transformation of cresol to toluene occurs at a faster rate than the acid-catalyzed condensation reaction, thus forming a more stable compound and consequently decreasing the rate of light hydrocarbons formation. It is important to emphasize that each reaction involves several steps and different catalytic functions. For example, the m-cresol dehydroxilation to toluene involves a first hydrogenation step on the metal and then the dehydration on the acid [48]. According to the activity results shown above, the metal function controls the reaction rate of m-cresol dehydroxylation.

The methylcyclohexane/toluene (MCH/Tol) ratio was practically the same in all four catalysts The benzene/toluene ratio decreased as the Pt loading increased, being 0.1 for the Pt(0.5%) and 0.01 for the Pt(1.7%) (data from Table 5). Even though, under the conditions used to obtain the data shown in this table the conversion was 100%, this large difference between the two catalysts indicates that there is a significant difference in the relative rates of dehydroxylation and demethylation, as the metal content increased. As the Pt loading increased, the reaction rate of dehydroxylation forming toluene increased relative to the rate of demethylation forming phenol and then benzene. To verify this behaviour, experiments were carried out changing the W/F and the H_2/m-cresol ratio in order to obtain conversions lower than 100%. Results are shown in Table 6. It was possible to measure the activity with conversions in the order of 80%, although working with very different W/F and H_2/m-cresol ratios. It is important to highlight that the toluene selectivity increases as the metal content increased, in agreement with results shown in Table 5 using other reaction conditions. The benzene/toluene ratio also follows the same trend as that shown in Table 5, i.e., it decreased as the metal content increased, except in the case of the Pt(0.05%) catalyst in which, due to the high selectivity to light hydrocarbons, the benzene production was negligible.

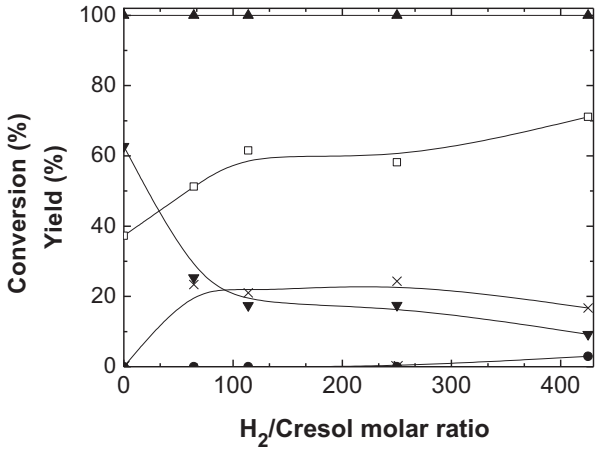

Fig. 6. Cresol conversion and product yield vs. H_2/cresol molar ratio. Catalyst: Pt(1.7%)/γAl_2O_3 at 300 °C, P = 1 bar, W/F = 6.4 $g_{cat}\,h\,(g_{cresol})^{-1}$. References: (▲) m-cresol conversion, (□) toluene, (×) LH, (▼) benzene, (▷) phenol, and (●) methylcyclohexane.

In summary, as the metal content increased, the deoxygenation reaction of m-cresol to toluene became the main reaction path, being faster than both, the demethylation of cresol to phenol, and the condensation followed by hydrocracking reactions.

3.6. Effect of the H_2/cresol ratio on the product yields and stability

The effect of the H_2/cresol ratio on the product yields was studied at 300 °C on Pt(1.7)/γAl_2O_3. The W/F was 6.4 $g_{cat}\,h\,(g_{cresol})^{-1}$ and the H_2/cresol ratio was varied by changing the H_2 partial pressure in a current of N_2, and keeping constant the total flow rate at 30 mL min^{-1}. The conversion and product yields, after 20 min of reaction, are shown in Fig. 6. The coke deposited on the catalyst after 2.25 h of reaction was determined by TPO (see Table 7).

Table 7
Value of %C obtained for spent Pt(1.7%)/γAl_2O_3 catalyst at different H_2/cresol molar ratios and W/F 6.4 $g_{cat}\,h\,(g_{cresol})^{-1}$.

H_2/cresol molar ratio	H_2 partial pressure	%C
0	0.00	1.50
64	0.13	1.22
114	0.22	0.80
250	0.50	0.40
425	0.83	0.33

The higher the H_2/cresol ratio, the lower the amount of carbon deposited on the catalyst. Fig. 6 shows that toluene yield was higher and benzene yield was lower as H_2/cresol ratio increased. Methylcyclohexane was observed only at the highest H_2/cresol ratio. These results makes it possible to conclude that as hydrogen partial pressure increases, the hydrodeoxygenation rate (forming toluene) increases relative to the demethylation reaction (forming phenol). Because of this, lower amount of benzene was observed at higher H_2/cresol ratio, since as indicated by the results shown in Figs. 4 and 5 the rate of toluene transformation to benzene is slower than the phenol dehydroxylation to benzene.

3.7. Effect of temperature on product selectivity

Conversion levels and product yields at different temperatures were analyzed using Pt(1.7)/γAl_2O_3 catalyst. Results obtained while increasing the temperature are shown in Fig. 7A. The yields obtained at each temperature while decreasing its value were not exactly the same as those obtained while increasing the temperature, indicating that there was deactivation. Three temperature ranges can be clearly distinguished. In the lower temperature range (below 250 °C), the main product was methylcyclohexane. Dehydroxylation also occurred in the lower temperature range, but no hydrocracking took place. In the intermediate temperature range (250–350 °C) the cresol dehydroxylation was favoured, being toluene the main product; and in the higher temperature range (above 350 °C), benzene and light hydrocarbons were the main reaction products. It is important to highlight that deactivation led to an increase in selectivity towards toluene, and a decrease towards light hydrocarbons and methylcyclohexane (compare Fig. 7A and B).

Methane was formed by the hydrocracking of cresol condensation products, leading to a methane yield higher than the benzene yield, as observed in the activity data obtained while increasing the temperature. It can be concluded that the cresol deoxygenation reaction can be successfully carried out at different temperature levels and atmospheric pressure, according to the desired products.

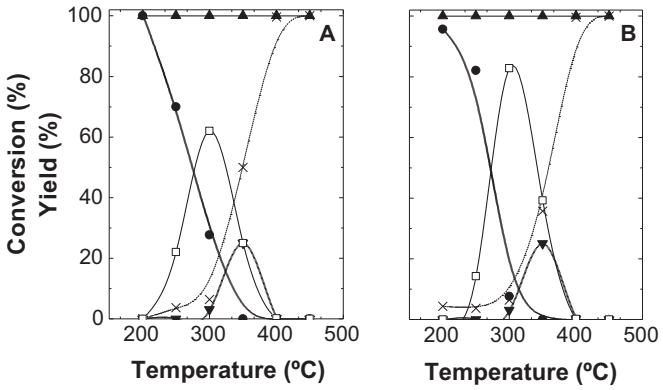

Fig. 7. Cresol conversion and product yield vs. temperature. Catalyst: Pt (1.7)/γAl_2O_3. W/F = 37.7 g_{cat} h ($g_{reactants}$)$^{-1}$. (A) Increasing temperature from 200 to 450 °C. (B) Decreasing temperature from 450 to 200 °C. References: (▲) m-cresol conversion, (□) toluene, (×) LH, (▼) benzene, (▷) phenol, and (●) methylcyclohexane.

3.8. Cresol deoxygenation routes. Catalyst stability

The reaction routes proposed for m-cresol deoxygenation are shown in Scheme 1, in which each step may involve one or more intermediates not observed in this study due to their very low concentrations in the gas phase. Toluene is formed by dehydroxylation of cresol. Phenol is formed by hydrogenolysis of the cresol methyl group. Two different routes generate benzene. Hydrogenolysis of toluene methyl group produces benzene and methane, while dehydroxylation of phenol forms benzene. The latter reaction can occur both on the metal and on the acid sites [48]. It has been proposed

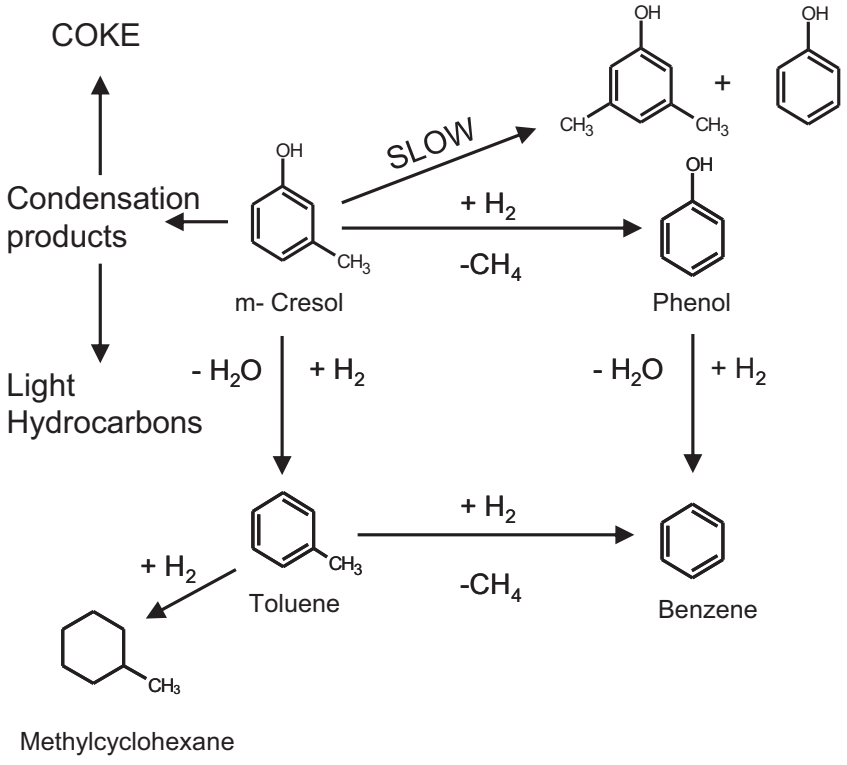

Scheme 1. Proposed reaction routes for m-cresol deoxygenation over Pt/γAl_2O_3.

that this reaction occurs on the metal after the aromatic ring is partially hydrogenated, and then the C—O bond breakage occurs followed by dehydrogenation of the ring [47]. The hydrogenolysis of the toluene methyl group was confirmed by feeding toluene to the reaction system. In this reaction, benzene and methylcyclohexane were found as the reaction products, although benzene appeared in very low amounts. The other reaction path for benzene formation, i.e. phenol dehydroxylation, was confirmed by feeding the mixture of phenol and cresol. This reaction was compared with the reaction carried out under the same conditions but feeding only cresol. As seen in Fig. 4, the benzene/toluene ratio for the same conversion level was much higher when feeding the mixture phenol–cresol, confirming that benzene was also formed from phenol but at a higher rate than the demethylation of toluene. Finally, methylcyclohexane was formed by hydrogenation of toluene.

The conversion levels were 100% for contact times between 37.7 and 4.34 $g_{cat}h(g_{cresol})^{-1}$ (Fig. 3). However, the product yield changed with time on stream, indicating the progressive catalyst deactivation. In all cases it was observed that as the reaction proceeded, benzene and methane yields decreased while toluene yield increased. A significant amount of methylcyclohexane was only observed for the highest contact time. As the reaction proceeded, carbon deposits were formed both on metal and acid sites and, consequently, the benzene and methylcyclohexane yields decreased. Besides, the coplanar type adsorption needed in order to hydrogenate toluene to methylcyclohexane was also more difficult as coke deposition occurred. It is very important to highlight that according to the TPO profile, coke was formed mainly on the metal particles, and therefore, the observed deactivation might be related to the activity loss of the metallic function. Other products found by GC–MS in low amounts were dimethyl diphenyl and dimethyl benzophenone. Methyl groups from these compounds can be hydrocracked, and because of this the light hydrocarbon fraction (which contained an important amount of methane) yield was higher than the benzene yield. According to these results, the secondary hydrocracking reactions deactivated faster than the cresol dehydroxylation reaction. Therefore, as the reaction proceeded less methane was produced and its yield (not shown) followed the same trend as the benzene yield.

4. Conclusions

Cresol deoxygenation was successfully carried out with $Pt/\gamma Al_2O_3$ catalysts at atmospheric pressure; toluene, benzene and methylcyclohexane being the main reaction products depending upon the reaction conditions. The yield of the desired product can be regulated by changing the metal loading, the H_2/cresol ratio and the reaction temperature. The toluene hydrogenation to methylcyclohexane is favoured at low temperature, while the toluene yield has a maximum at the intermediate temperature levels (around 300 °C), since at high temperatures toluene is transformed into benzene by demethylation. Catalyst deactivation is probably due mainly to cresol condensation products deposited on the catalyst surface. The amount of coke deposited during m-cresol deoxygenation on the $Pt/\gamma Al_2O_3$ is rather low, in the order of 1 wt.%, with an important fraction of coke formed on the metallic particles.

Acknowledgments

The authors wish to acknowledge the financial support received from ANPCyT, CONICET and CAID+D-UNL. Thanks are also given to Guillermo Pitich, Diego López Delzar and José Ignacio Lobos for the technical support, and to Elsa Grimaldi for the English language editing. Thanks are also given to ANPCyT for the purchase of the SPECS multitechnique analysis instrument (PME8-2003).

References

[1] Y. Sheu, R.G. Anthony, E.J. Soltes, Fuel Processing Technology 19 (1988) 31–50.
[2] E.G. Baker, D.C. Elliott, in: A.V. Bridgwater, J.L. Kuester (Eds.), Thermo chemical Biomass Conversion, Elsevier Application Sciences, London, UK, 1988, pp. 883–895.
[3] F.A. Agblevor, S. Besler, Energy & Fuels 10 (1996) 293–298.
[4] W. Craig, E. Coxworth, in: C. Granger, B.C. Richmond (Eds.), Proceedings of the Sixth Canadian Bioenergy R&D Seminar Canada, Elsevier Application Sciences, London, 1987, pp. 407–411.
[5] R. Maggi, B. Delmon, in: A.V. Bridgwater (Ed.) Advances in Thermochemical Biomass Conversion, London, 1993, 1185 pp.
[6] R. Maggi, A. Centeno, B. Delmon, Biomass energy environment, in: P. Chartier (Ed.), Proceedings of the 9th European Bioenergy Conference, Elsevier, Oxford, 1996, p. 327.
[7] P. Grange, A. Centeno, R. Maggi, B. Delmon, Thermochemical biomass process, in: A.V. Bridgwater, E.N. Hogan (Eds.), Bio-oil Prod. Util. Proc. EU-Can Workshop Therm Biomass Process 2nd 1995, CPL Press, Newbury, 1996, p. 186.
[8] C.A. Fisk, T. Morgan, Y. Ji, M. Crocker, C. Crofcheck, S.A. Lewis, Applied Catalysis A-General 358 (2009) 150–156.
[9] Y. Wang, T. He, K. Liu, J. Wu, Y. Fang, Bioresource Technology 108 (2012) 280–284.
[10] J.D. Adjave, N.N. Bakhshi, Fuel Processing Technology 45 (1995) 161–183.
[11] S.P.R. Katikaneni, J.D. Adjave, N.N. Bakhshi, Energy & Fuels 9 (1995) 1065–1078.
[12] P.T. Williams, P.A. Horne, Fuel 74 (1995) 1839–1851.
[13] J.D. Adjave, N.N. Bakhshi, Fuel Processing Technology 45 (1995) 185–202.
[14] J.D. Adjave, S.P.R. Katikaneni, N.N. Bakhshi, Fuel Processing Technology 48 (1996) 115–143.
[15] F. Janssen, Catalysis Science Series (1999) 1–4.
[16] V.N. Bui, D. Laurenti, P. Afanasiev, C. Geantet, Applied Catalysis B-Environmental 101 (2011) 239–245.
[17] W. Wang, Y. Yang, H. Luo, T. Hu, W. Liu, Catalysis Communications 12 (2011) 436–440.
[18] Y. Romero, F. Richard, Y. Reneme, S. Brunet, Applied Catalysis A-General 353 (2009) 46–53.
[19] E. Odebunmi, D.F. Ollis, Journal of Catalysis 80 (1983) 56–64.
[20] R.K.M.R. Kallury, T.T. Tidwell, D.G.B. Boocock, D.H.L. Chow, Canadian Journal of Chemistry 62 (1984) 2540–2545.
[21] C.R. Lee, J.S. Yoon, Y-W. Suh, J-W. Choi, J-M. Ha, D.J. Suh, Y-K. Park, Catalysis Communications 17 (2012) 54–58.
[22] B. Yoosuk, D. Tumnantong, P. Prasassarakich, Fuel 91 (2012) 246–252.
[23] B. Yoosuk, D. Tumnantong, P. Prasassarakich, Chemical Engineering Science 79 (2012) 1–7.
[24] Y. Romero, F. Richard, S. Brunet, Applied Catalysis B: Environmental 98 (2010) 213–223.
[25] V.N. Bui, D. Laurenti, P. Delichere, C. Geantet, Applied Catalysis B: Environmental 101 (2011) 246–255.
[26] Eun-Jae Shin, M.A. Keane, Industrial & Engineering Chemistry Research 39 (2000) 883–892.
[27] J.D. Adjaye, N.N. Bakhshi, Biomass & Bioenergy 8 (3) (1995) 131–149.
[28] P.D. Chantal, S. Kaliaguine, J.L. Grandmaison, Applied Catalysis. 18 (1985) 133–145.
[29] A.G. Gayubo, A.T. Aguayo, A. Atutxa, R. Aguado, J. Bilbao, Industrial & Engineering Chemistry Research 43 (2004) 2610–2618.
[30] A.G. Gayubo, A.T. Aguayo, A. Atutxa, R. Aguado, J. Bilbao, Industrial & Engineering Chemistry Research 43 (2004) 2619–2626.
[31] R.N. Olcese, M. Bettahar, D. Petitjean, B. Malaman, F. Giovanella, A. Dufour, Applied Catalysis B-Environmental 115-116 (2012) 63–73.
[32] M.A. González-Borja, D.E. Resasco, Energy & Fuels 25 (2011) 4155–4162.
[33] J. Filley, C. Roth, Journal of Molecular Catalysis A: Chemical 139 (1999) 245–252.
[34] A. Ausavasukhi, Y. Huang, A.T. To, T. Sooknoi, D.E. Resasco, Journal of Catalysis 290 (2012) 90–100.
[35] P.C. Aben, Journal of Catalysis 10 (1968) 224–229.
[36] M.G. White, Heterogeneous Catalysts, Prentice Hall, Englewood Cliffs, NJ, 1991, pp. 88.
[37] S.C. Fung, C.A. Querini, Journal of Catalysis 138 (1992) 240–254, 48.
[38] C. Meephoka, C. Chaisuk, P. Samparnpiboon, P. Praserthdam, Catalysis Communications 9 (2008) 546–550.
[39] M.J. Tiernan, O.B. Finlayson, Applied Catalysis B-Environmental 19 (1998) 23–35.
[40] A.C.S.F. Santos, S. Damyanova, G.N.R. Teixeira, L.V. Mattos, F.B. Noronha, F.B. Passos, J.M.C. Bueno, Applied Catalysis A-General 290 (2005) 123–132.
[41] J.C. Serrano-Ruiz, G.W. Huber, et al., Journal of Catalysis 241 (2) (2006) 378–388.
[42] A.S. Ivanova, E.M. Slavinskaya, et al., Applied Catalysis B: Environmental 97 (1–2) (2010) 57–71.
[43] A.K. Talukdar, K.G. Bhattacharyya, Applied Catalysis A-General 96 (1993) 229–239.
[44] J. Barbier, E. Churin, P. Marecot, Journal of Catalysis 126 (1990) 228–234.

[45] J. Barbier, in: G.F. Forment, B. Delmon (Eds.), Catalyst deactivation, Elsevier, Amsterdam, 1987, p. 1.
[46] J. Barbier, E. Churin, J.M. Parera, J. Riviere, Reaction Kinetics and Catalysis Letters 29 (1985) 323–330.
[47] R. Taylor, K.H. Lundlum, Journal of Physical Chemistry 76 (1972) 2882–2886.
[48] P.T.M. Do, A.J. Foster, J. Chen, R. Lobo, Green Chemistry 14 (2012) 1388.
[49] A.J. Foster, P.T.M. Do, R. Lobo, Topics in Catalysis 55 (2012) 118–128.
[50] H. Huang, R.V. Chaudhari, B. Subramaniam, Topics in Catalysis 55 (2012) 129–139.